ENDOCRINE SOCIETY

ADVANCE ARTICLE: JES JOURNAL OF THE ENDOCRINE SOCIETY

Information Transfer via Gonadotropin-Releasing Hormone Receptors to ERK and NFAT: Sensing GnRH and sensing dynamics.

Kathryn L. Garner, Margaritis Voliotis, Hussah Alobaid, Rebecca M. Perrett, Thanh Pham, Krasimira Tsaneva-Atanasova and Craig A. McArdle

Journal of the Endocrine Society
Endocrine Society

Submitted: December 15, 2016
Accepted: February 22, 2017
First Online: February 28, 2017

Journal of the Endocrine Society; Copyright 2017 DOI: 10.1210/js.2016-1096

Information Transfer via Gonadotropin-Releasing Hormone Receptors to ERK and NFAT: Sensing GnRH and sensing dynamics.

Kathryn L. Garner[1], Margaritis Voliotis[2,3], Hussah Alobaid[1], Rebecca M. Perrett[1], Thanh Pham[4], Krasimira Tsaneva-Atanasova[2,3] and Craig A. McArdle[1]

[1]Laboratories for Integrative Neuroscience and Endocrinology, School of Clinical Sciences, University of Bristol, Bristol, BS13NY, UK. [2]EPSRC Centre for Predictive Modelling in Healthcare, University of Exeter, EX44QF, UK. [3]Department of Mathematics, College of Engineering, Mathematics and Physical Sciences, University of Exeter, Exeter, EX44QF, UK. [4]Texas A and M University Corpus Christi, Corpus Christi, Texas 78412, USA.

Received 15 December 2016. Accepted 22 February 2017.

Information theoretic approaches can be used to quantify information transfer via cell signaling networks. Here we do so for gonadotropin-releasing hormone (GnRH) activation of ERK (extracellular signal-regulated kinase) and NFAT (nuclear factor of activated T-cells) in large numbers of individual fixed LβT2 and HeLa cells. Information transfer, measured by mutual information between GnRH and ERK or NFAT, was <1Bit (in spite of 3 Bit system inputs). It was increased by sensing both ERK and NFAT but the increase was <50%. In live cells information transfer via GnRH receptors to NFAT was also <1Bit and was increased by consideration of response trajectory, but the increase was <10%. GnRH secretion is pulsatile so we explored information gained by sensing a second pulse, developing a model of GnRH signaling to NFAT with variability introduced by allowing effectors to fluctuate. Simulations revealed that when cell-cell variability reflects rapidly fluctuating effector levels, additional information is gained by sensing two GnRH pulses but where it is due to slowly fluctuating effectors, responses in one pulse are predictive of those in another, so little information is gained from sensing both. Wet-lab experiments revealed that the latter scenario holds true for GnRH signaling; within the timescale of our experiments (1-2hr) cell-cell variability in the NFAT pathway remains relatively constant so trajectories are reproducible from pulse to pulse. Accordingly, joint sensing, sensing of response trajectories and sensing of repeated pulses can all increase information transfer via GnRHR but in each case the increase is small.

Information transfer via GnRHR is increased by joint sensing of ERK and NFAT and by sensing trajectories but the increases are small as most information is lost through these noisy signaling pathways.

INTRODUCTION

Single cell measures of cell signaling pathways and proteins reveal marked cell-cell variation but relatively little is known about the biological relevance of this heterogeneity. It is, in fact, inevitable because the processes underlying signaling are stochastic, and is thought to be crucial for the behaviour of cell populations (1) where each individual cell has to sense the environment and make appropriate decisions (to express or suppress given genes, for example). Information theoretic approaches are increasingly being applied to cell biology, where cell signaling systems can be treated as noisy communication channels and statistical measures of information transfer that take into account cell-cell variation can be calculated (1-8). Here, information is defined as the uncertainty about the environment that is reduced by signaling, and is measured as the Mutual Information (MI) between two stochastic variables describing the signal and the response (1). For cell signaling pathways, these variables could be the concentration of stimulus in the environment and the activity of an effector. In this case MI quantifies the quality of the inference of the signal from the response, providing a statistical measure of information transfer through the pathway.

This information theoretic approach takes variability into account rather than just considering the average response, can be applied to any cell signaling system in which signal and response are known, and can provide significant additional insight into cell signaling. Its merit can be illustrated by consideration of a signaling network with multiple possible routes of information transfer, as it would theoretically be possible to measure the amount of information passing from any given receptor to any given effector. The network may well contain numerous potential drug targets but the pathways and effectors providing the cell with most information about the environment would presumably make the most attractive targets for therapeutic manipulation. Alternatively, for a simpler multi-tiered signal-transduction pathway it is often assumed that signal amplification occurs through the cascade. However, information theory tells us information about the signal cannot actually increase from one tier to the next so any increase in numbers of activated molecules must be associated with increased variability. In fact, there is almost inevitably loss (and never gain) of information through such cascades. Indeed, marked loss of information has already been documented for several signaling pathways including for tumour necrosis factor (TNF) signalling to NFκB (2), for nerve growth factor (NGF) and pituitary adenylyl cyclase-activating polypeptide (PACAP) signaling to cyclic AMP-response element binding protein (CREB), c-FOS and Egr1 (7) and for epidermal growth factor (EGF) signaling to ERK (4). In each of these cases approximately 3 Bits of information were available (i.e. $\sim 2^3$ states of the environment were considered) but <1 Bit of information was typically transferred. This raises the question of how cells could mitigate this loss and emphasis has been placed on negative feedback loops that could reduce information transfer by reducing dynamic range of the output, or increase it by reducing cell-cell variability or by preventing basal stimulation due to constitutive protein activity (2,4,9).

Here, we explore information transfer via gonadotropin-releasing hormone receptors (GnRHR) to ERK. GnRHR are $G_{q/11}$ coupled G-protein coupled receptors (GPCRs) in the pituitary that mediate central control of reproduction (10). When activated by the neuropeptide GnRH they cause a phospholipase C (PLC)-mediated increase in the cytoplasmic Ca^{2+} concentration that drives exocytotic gonadotropin secretion. This Ca^{2+} elevation also has marked effects on transcription, in part mediated by the Ca^{2+}/calmodulin-mediated activation of NFAT (nuclear factor of activated T-cells) (10,11). GnRHR-mediated PLC activation also activates protein kinase C (PKC) isozymes and causes a (largely) PKC-mediated activation of ERK and of ERK-driven transcriptional responses (10,12-18). Where single cell measures are available they typically reveal marked cell-cell variability, even in clonal cell models. Thus, GnRH effects on cytoplasmic Ca^{2+} concentration, gonadotropin secretion, effector activation and gene expression all show pronounced heterogeneity in normal pituitary cells as well as in gonadotrope-lineage cell lines and in heterologous receptor expression systems (9,11,17-24). Using a high content imaging system to obtain signaling measures from large numbers of individual cells and MI to quantify GnRH sensing, we recently showed that there was a marked loss of information through signaling in that, for most experiments there were 3 Bits of information available but information transfer was always <1 Bit. Here we address a number of possible reasons for this low level of information transfer. We test the relevance of cellular context and effector choice by quantifying MI between GnRH and ppERK or NFAT using upstream and transcriptional readouts in HeLa cells and in LβT2 (gonadotrope-lineage) cells. We also address the possibility that additional information is gained by joint sensing of both of these pathways or by sensing response trajectories over time, using wet-lab data and by developing a hybrid mechanistic/probabilistic model of GnRH signaling to NFAT. Our key findings are that information transfer can indeed be increased by joint sensing (of ERK and NFAT) and by sensing NFAT over time but in each case the additional information gained is relatively small. Indeed, MI values were <1 Bit under all conditions considered, suggesting that most information about GnRH concentration is actually lost by GnRH-responsive cells such that these individual cells cannot unambiguously distinguish between even two states of the environment.

MATERIALS AND METHODS

Cell culture and transfection.

The murine gonadotrope-derived LβT2 cell line was kindly provided by Prof. PL Mellon (UCSD, CA, USA). The cells were routinely cultured in Dulbecco's Modified Eagle medium (DMEM), 10% heat inactivated foetal calf serum (FCS) (Gibco), 100 units/ml penicillin and 0.1mg/ml streptomycin (Sigma-Aldrich) in Matrigel Basement Membrane Matrix (Becton Dickinson)-coated tissue culture flasks and were plated (10 x10^3 cells/well) in Costar black-walled 96-well plates (Corning) for imaging experiments. For most experiments the plated cells were also transduced with recombinant adenovirus (Ad) for expression of an NFAT1c-EFP translocation reporter (11). Approximately 16 hr after plating they were incubated 4-6hr in DMEM/2% FCS with Ad NFAT1c-EFP. The medium was then replaced with DMEM/0.1% FCS and the cells were incubated for a further 16 hr before stimulation as described (18). For some experiments imaging readouts for pathway-specific transcriptional responses were obtained by transducing cells with Ad for expression of an Egr1 promoter driving expression of zsGREEN (Ad Egr1-zsGREEN) or with Ad for expression of an NFAT response element driving expression of asRED (Ad NFAT-RE asRED) as described (25). As an alternative cellular model HeLa cells (from ECACC) were used. They were cultured, plated and transduced as described (25,26) and, since HeLa cells do not express endogenous GnRHR, they were also transduced with Ad GnRHR as described (25-28). In this model GnRHR number is dependent on Ad titre and Ad GnRHR was used at 1-2 plaque-forming units (pfu)/nl to provide receptor expression at approximately 50,000 sites/cell (9) which is within the range of 20,000–75,000 sites/cell estimated for endogenous GnRHR in gonadotrope lineage cells and primary cultures (9,29). All other Ad were used at 1-10 pfu/nl and stimulation details are given in the figure legends.

Image acquisition and analysis.

For the first experiments LβT2 cells or Ad GnRHR transduced HeLa cells were stimulated for varied periods with varied concentrations of GnRH before being fixed and stained with DAPI (4'-6-diamidino-2-phenylindole) for visualisation of nuclei and with anti-ppERK antibody (Sigma-Aldrich Cat# M9692, RRID:AB_260729) followed by Alexa Fluor® goat anti-mouse fluorescent secondary antibody (Molecular Probes) (25-28). Digital images were then acquired with an InCell Analyzer 1000 high content imaging platform (GE Healthcare) using a 10x objective and filters for DAPI (blue channel) and Alexa488 (green channel, Thermo Fisher Scientific Cat# A-11029, RRID_2534088) or Alexa546 (red channel, Thermo Fisher Scientific Cat# A-11030, RRID:AB_2534089). For some experiments NFAT1c-EFP, zsGREEN or asRED were also visualised (using green and red channel filters as appropriate). Automated image analysis was as described (27) determining whole cell or nuclear fluorophore intensities in arbitrary fluorescence units (AFU). For the NFAT1c-EFP translocation assay background-subtracted cytoplasmic and nuclear fluorescence intensities were used to calculate the fraction of

NFAT1c-EFP in the nucleus (NFAT-NF, nuclear fraction). Replicate treatments in 2-4 wells of cultured cells were pooled to produce population-averaged responses that were pooled from multiple experiments ppERK (25-28).

For live cell imaging experiments, HeLa cells cultured, plated and transduced with Ad GnRHR and Ad NFAT1c-EFP as above were transferred to live cell imaging buffer (20mM HEPES pH7.4, 137mM NaCl, 5mM KCl, 2mM $MgCl_2$, 1.8mM $CaCl_2$, 5.6mM glucose, 1mg/ml BSA, 0.5mM NaH_2PO_4, 1mM $NaHCO_3$, 0.03mM phenol red) and stained with Hoechst 33342 dye (Molecular Probes) for 30 min equilibration, serum starvation and nucleus staining. The cells were imaged at 37^{o}C both before and during stimulation with GnRH (0, 10^{-11}, 10^{-9} or 10^{-7}M). For the first live cell imaging experiment the cells received a single 60 min pulse of GnRH, but for the second experiment there were two pulses; a 15 min pulse terminated by extensive washing (4 changes of medium) followed by an interval of 135 min and a subsequent 60 min pulse of GnRH (at the same concentration as had been used for the first pulse). Digital images were acquired (at the time points indicated in the figures) and individual cells were tracked over time (below) so that NFAT-NF could be plotted against time for each individual tracked cell. These individual cell time-courses were inspected for removal of cells in which tracking had failed and outliers with time 0 NFAT-NF values <0.4 or >0.55 (this removed <10% of the cells from 3 repeated experiments). The figures show representative individual cell responses, as well as population averaged responses for all tracked cells.

Data analysis.

For the initial fixed cell experiments we constructed full concentration response curves (i.e. control and 10^{-12}–10^{-6} M GnRH) at multiple time points and collected images for 4-9 fields of view per well. This yielded measures of nuclear ppERK or NFAT-NF for >10,000 individual cells (for each treatment in each experiment). For some experiments GnRH potency was estimated by curve fitting of population average responses using GraphPad Prism (log [agonist] versus response, four parameter fit using Prism 6 for Windows, version 6.05). In addition, for most experiments individual cell measures from complete concentration-response curves were used to calculate MI between stimulus concentration and the experimental measure at each time point. MI was estimated using the following formula:

$$I(Z;S) = H(Z) - H(Z|S)$$

where I is the mutual information between a signal (S) and a response (Z), H(Z) is the unconditional entropy of the response, and $H(Z \mid S)$ is the conditional entropy (4). To estimate these entropy terms we used the Bayesian method proposed by Nemenman *et. al.* (30), which also provides error bars for these estimates. As the method is designed for discrete data, we discretised ERK and NFAT cell measures by binning them into 30 equally sized bins.

For the second series of fixed cell experiments, data were collected (as above) for nuclear ppERK and NFAT-NF in the same cells, or for Egr1-driven zsGREEN and NFAT-RE-driven asRED, again in the same cells. This enabled us to calculate not only the MI between GnRH and each individual experimental measure but also the joint MI between GnRH and the paired outputs (ppERK and NFAT-RE or asRED and zsGREEN) as above, but with response (Z) now interpreted as a two-dimensional vector.

For the live cell imaging experiments, cells were initially segmented from the DAPI images using InCell Analyzer software. Individual cells were then tracked by matching the geometric centres of the nuclei between successive images in the time stack. Cells were paired with probability that depended exponentially on their Euclidean distance and Markov-Chain Monte-Carlo was used to find the most likely matching configuration for each pair of images.

For the single pulse live cell imaging experiments MI values were then calculated between GnRH and the NFAT-NF translocation response at individual time points. In addition MI values were calculated between GnRH and the integral of the NFAT-NF translocation response (over the 60min stimulation period) or using 3 time-points to take response trajectory into consideration. For the dual pulse live cell imaging experiments the responses (Z_1 and Z_2) to the 1st and 2nd pulse were measured as the maximum NFAT-NF value during each pulse. Information $I(Z_1;GnRH)$ was calculated while the additional information from the response to the 2nd pulse was calculated using the following formula

$$I(Z_1;S|Z_1) = I(Z_1;GnRH) - I(Z_1;Z_2) + I(Z_1;Z_2|GnRH)$$

where $I(Z_1;Z_2)$ is the MI between the individual cell responses in pulse 1 and 2 and $I(Z_1;Z_2 \mid GnRH)$ and the MI between the individual cell responses in pulse 1 and 2 conditioned on the concentration of GnRH.

All of the analysis was performed in MatLab (MathWorks, Natick, MA, USA).

Simulations of the hybrid (deterministic/stochastic) model.
We used a deterministic model of GnRH signaling that was adapted from an earlier version (31) by removal of the ERK signaling pathway and transcription regulation steps and by altering the NFAT translocation parameters to better fit the response dynamics shown for wet-lab data in Fig.6. We introduced stochastic dynamics for two effectors in the model, GnRHR (the first step in the pathway) and calmodulin (CaM, which equates to parameter M in (31)), by allowing the corresponding parameters (describing the total amount of these effectors) to fluctuate over time according to an exponentiated Ornstein-Uhlenbeck process: with stationary mean set to the value of the corresponding parameter in the deterministic model; stationary variance set such that the response variability matches the one observed experimentally; and fluctuation lifetime (FL) varied between 10 min (unstable effector) and 10000 min (stable effector). We used the hybrid model to simulate responses to two pulses of 0, 10^{-11}, 10^{-9} and 10^{-7} M GnRH. The first pulse was for 15 min and this was followed by a 135 min interval and then a second pulse (of 60 min). As with the wet-lab data, we measured the responses to the 1st and 2nd pulse (Z_1 and Z_2) as the maximum NFAT-NF value during each pulse. We ran simulations for 1000 cells at each GnRH concentration/FL combination, and used the simulated responses to calculate $I(Z_1;GnRH)$ and the additional information from Z_2 as detailed above.

RESULTS

Statistical measurement of information transfer via GnRHR to ERK and NFAT.
LβT2 were stimulated continuously with varied concentrations of GnRH for 5, 15, 30, 60, 120 or 240 min before staining and imaging. Image analysis revealed that GnRH caused the expected rapid (maximal or near maximal at 5 min) and concentration-dependent increases in ppERK (Fig.1A, (9,17,24)). The population-averaged data shown are derived from $>10^6$ cells, and representative frequency distribution plots are shown in Supplemental Fig.1C. The single cell data for each of the GnRH concentration-response curves was used to calculate MI between GnRH and ppERK (I(ppERK;GnRH) and this value increased rapidly to approximately 0.7 Bits at 5 min with a gradual reduction to ~0.5 Bits at 240 min (Fig.1B). Similar experiments were undertaken with LβT2 cells transduced with Ad NFAT-EFP before staining, imaging and calculation of the NFAT nuclear fraction (NF). Again, GnRH caused a concentration-dependent increase in NFAT-NF (Fig. 1C) that was slower than the effect on ppERK (maximal or near maximal at 60 min). Frequency-distribution plots are shown in Supplemental Fig.1D and the

single cell measures were used to calculate MI between GnRH and NFAT-NF. As shown (Fig.1D), information transfer to NFAT was lower than to ERK as I(NFAT-NF;GnRH) values were lower, increasing to a maximum (~0.3 Bits) at 60 min with a gradual reduction toward 240 min. For clarity, the data in Figs.1A and 1C are replotted against time in Supplemental Fig.1 and this reveals that the population averaged ppERK response to GnRH was more sustained with the higher concentrations of GnRH than with10^{-11}-10^{-9} M GnRH. This reflects the time-dependent rightward shift in the GnRH concentration-response curves evident in Fig.1A (i.e. the EC_{50} for GnRH was approximately 1 nM at 5 min and 46 nM at 240 min, see Fig.1 legend for all EC_{50} values). Here, it is important to recognise that all of the individual cell measures underlying the full concentration-response curves were used for the MI calculations, and that these MI values would not be expected to be influenced by the time-dependent reduction in GnRH potency (as measured by EC_{50} values) so long as the GnRH concentrations used encompass the full dynamic range of the response. Accordingly, these data collectively reveal that MI can be used to measure information transfer via endogenous GnRHR to ERK and NFAT, and that for each output and time-point considered, the MI values approximately paralleled the dynamic range observed for the population averaged responses.

Joint sensing of ERK and NFAT signaling.
In the experiments above MI values were always <1Bit in spite of system inputs of 3 Bits (i.e. 2^3 different GnRH concentrations). This implies that most information from the environment is lost through signaling, but an important alternative possibility is that sensing of multiple pathways within the network actually mitigates any such loss. We addressed this by measuring ERK phosphorylation and NFAT translocation responses in the same population of Ad NFAT-EFP transduced LβT2 cells. As shown (Fig.2), GnRH caused the expected concentration-dependent and time-dependent increases in ppERK and NFAT-NF with very similar I(ppERK;GnRH) values (~0.5 Bits) at 5, 20 and 60 min, whereas I(NFAT-NF;GnRH) values increased from 5 to 60 min. Joint MI values were comparable at all time-points and were always greater than MI values for either response alone, but the increase was modest (maximally from ~0.5 to ~0.7) so the additional information gained by joint sensing was small. Similar experiments were performed with cells transduced with Ad Egr1-zsGREEN and Ad NFAT RE-asRED (as imaging readouts for ERK-driven and NFAT-driven transcription, respectively) and stimulated for 4, 6 or 8 hr before imaging. Again, GnRH caused concentration- and time-dependent increases in expression of both reporters although as expected these responses were much slower (note the different time points used for the upper and lower panels in Fig.2). MI values were approximately 0.8 at all 3 time points for the Egr1-reporter and were considerably lower (0.2-0.3 Bits) for the NFAT-RE reporter. Joint MI values were greater than for either reporter alone but the increase was modest (from ~0.8 to ~0.9 Bits) so although additional information is gained by sensing both effectors, this increase was again small. Similar experiments were undertaken with HeLa cells and this yielded similar conclusions (Supplemental Fig.2). Joint MI values were greater than for I(ppERK;GnRH) and I(NFAT-RE;GnRH) but the increase was small (i.e. from ~0.7 to ~0.8 Bits for 5 min responses) and although joint MI values were greater than for I(Egr1-zsGREEN;GnRH) or I(NFAT-RE-asRED;GnRH) the increase was again small (i.e. from ~0.35 to ~0.45 Bits for 8 hr responses). Interestingly, these experiments also revealed signal bias for information transfer in these two models. GnRH tended to cause more sustained increases in ppERK in LβT2 cells than in Ad GnRHR-transduced HeLa cells (compare Fig.2A and Supplemental Fig.2A, particularly at the maximally effective concentrations). Since transcriptional effects of ERK are most pronounced with sustained stimulation (32), it is not

surprising that GnRH had a more pronounced effect on Egr1-zsGREEN expression in LβT2 cells than it did in HeLa cells (compare Fig.2D with Supplemental Fig.2D). There was also more information transfer in LβT2 cells as I(Egr1-zsGREEN;GnRH) was ~0.8 Bits in LβT2 cells and only ~0.2 Bits in HeLa cells (compare Fig.2F and Supplemental Fig.2F). In contrast, for the NFAT-driven transcriptional response as I(NFAT-RE-asRED) values were lower in LβT2 cells than in HeLa cells (compare panels E and F in Fig.2 and Supplemental Fig.2). Together these data reveal that in Ad GnRHR transduced HeLa cells, more information about GnRH concentration is transferred to the transcriptome via NFAT than viaERK, but that the opposite is true in LβT2 cells. Moreover, for both cell types information transfer is increased by joint sensing of NFAT and ERK although this additional information is very small (always <50%).

Sensing response trajectories.
The data above were obtained by imaging fixed cells and such "snap-shot" data may well underestimate the information available to cells sensing response trajectories over time. We addressed this for the Ca^{2+}/calmodulin/calcineurin/NFAT pathway by live cell imaging of Ad NFAT-EFP and Ad GnRHR-transduced HeLa cells and cell tracking. As shown (Fig.3), the responses of individual cells to GnRH were highly variable with some cells showing rapid and sustained increases in NFAT-NF (red shade traces in Fig.3A) whereas some showed little or no response (grey shade traces in Fig.3A) and others showed rapid and transient responses (blue shade traces in Fig.3B) or delayed responses (red traces in Fig.3B). The rapid and sustained responses were most prevalent (>50-75%) whereas very few cells showed delayed responses (3/166 for this data set). The population averaged responses increased to maxima at 15-60 min (Fig.3C) and MI between GnRH and NFAT-NF was ~0.5 Bits at all time-points measured. These data demonstrate that we have not underestimated I(NFAT-NF;GnRH) by missing a specific time-point and are broadly consistent with the snap-shot data shown (for 5, 20 and 60 min) in Supplemental Fig.2. Using the live cell data we could also calculate I(NFAT-NF;GnRH) using the area under the curve for the tracked cell responses (I(NFAT-NF AUC;GnRH)) or using 3 time points (I(NFAT-NF trajectory;GnRH)) and these values were ~0.52 and ~0.55 Bits, respectively (as compared to an average of 0.48 for the snap-shot data). Accordingly, although sensing of response trajectory can theoretically increase the MI values, sensing over time provided little or no increase in information transfer via GnRHR to NFAT.

Sensing GnRH pulses.
Physiologically GnRH is secreted in pulses and signaling can continue beyond the GnRH pulse (33) raising the question of how much information is gained by sensing during and after the pulse. We initially addressed this theoretically by developing a hybrid (deterministic/stochastic) model for GnRH signaling to NFAT. To do so we simplified a deterministic model of GnRH signaling that was adapted from an earlier version (31) by removal of the ERK signaling pathway and transcription regulation steps, and by altering the NFAT translocation parameters to better fit the response dynamics shown for wet-lab data in Fig.6. This was used to simulate responses during and immediately after a 15 min pulse of 0, 10^{-11}, 10^{-9} and 10^{-7} M GnRH. We introduced stochasticity into the concentration of two effectors: GnRHR and calmodulin. We allowed each of these to fluctuate, considering both unstable effector expression with a fluctuation lifetime (FL) of 10 min and stable effector expression with an FL of 10000 min. We ran simulations for 1000 cells at each combination of GnRH concentration and FL, so that MI values could be calculated. As expected (Fig.4), population averaged simulation data revealed NFAT-NF responses for the stable and unstable systems that had comparable means and variance (Fig.4A) in spite of the fact that individual cell response trajectories were more variable

(Fig.4B) with the more unstable effector concentrations (Fig.4C and D). The individual cell simulation data were used to calculate MI values using (as response) the AUCs of the individual cell traces either during the 15 min GnRH pulse or in the following 15 min. These values were comparable (i.e. 0.27±0.02 and 0.30±0.02 Bits during and after the GnRH pulse with FL10). As in live cell data above, MI values calculated using the snap-shot data were comparable to those calculated using response AUCs (Fig.4). Moreover, when we calculated the additional information gained by sensing both during and after the GnRH pulse (Fig.4, cross-hatched bars) this was low, but was greater for the unstable scenario (0.10±0.03 with FL=10 and 0.03±0.03 with FL=10000). Thus, these simulations suggest that for NFAT signaling, the cells can gain as much information about GnRH concentration after the pulse as they do within it, and that the additional information to be gained by sensing both would be greatest for conditions in which effector concentrations fluctuate rapidly.

The data described above are from a larger series of simulations in which we also considered the question of how much additional information can be gained by sensing a second GnRH pulse. Thus the full simulations included a 15 min pulse of GnRH followed by an interval of 135 min and then a second (60 min) pulse of GnRH at the same concentration as the first pulse. These simulations were run with four effector stabilities (FL=10, 100, 1000 and 10000 min) and again, population averaged NFAT-NF responses for the stable and unstable systems that had comparable means and variance (Fig.5A) in spite of the fact that individual cell response trajectories were more variable with the more unstable effectors (compare Fig.5B left and right hand panels). When effector stability is high the cells showing greatest responses in pulse 1 also show large responses in pulse 2, whereas this is not the case when effector stability is low (compare Fig.5B left and right hand panels). I(NFAT-NF;GnRH) values calculated using AUCs (for the first 15 min of stimulation in either pulse) were ~0.25-0.4 Bits and were comparable for pulse 1 and pulse 2 irrespective of effector stability (Fig.5C). Additional information gained by sensing both pulses was negligible with high effector stability but increased to >0.2 Bits at the lowest effector stability (Fig.5D). We also calculated the MI between the pulse 1 and pulse 2 responses and this increased from 0 to ~1.8 Bits as FL was increased from 10 to 10000 min (i.e. as effector stability increased). Thus, these simulations reveal that the additional information from the second pulse is dependent on the nature of the variation. If the heterogeneity reflected a broad distribution of effector concentrations that was constant over time, then the response in pulse 2 would be predictive of that in pulse 1 and there would be no additional information from sensing both. This is the situation approached at FL=10000 min where additional information from the second pulse is negligible and the MI between pulse 1 and 2 responses is high. In contrast, if the source of the heterogeneity was random or changed rapidly over time, the response in pulse 2 would be less predictive of that in pulse 1 so additional information would be obtained by sensing both. This is the scenario with FL= 10, where additional information from the second pulse is relatively high (Fig.5D) and the MI between pulse 1 and 2 responses is low (Fig.5E).

The simulations above illustrate conditions where additional information is, or is not, gained by sensing during and after one pulse, or by sensing two consecutive pulses, raising the question of what actually happens in GnRH-stimulated cells. To test this we stimulated Ad GnRHR and Ad NFAT-EFP transduced HeLa cells with two separate pulses of GnRH at 0, 10^{-11}, 10^{-9} and 10^{-7} M followed by imaging and individual cell tracking as outlined above. The first pulse was for 15 min and was terminated by washing (4 times) to remove the stimulus, followed by an interval of 135 min and then stimulation (60 min) with GnRH at the same concentration as had been used for the first pulse (Fig.6). I(NFAT-RE;GnRH) values calculated using the AUCs for the individual cell response during the first 15 min of each pulse were comparable to one-another (0.58 ±0.06 and 0.50±0.06 for pulse 1 and 2, respectively) and the values obtained in the single pulse experiment (Fig.3). An unexpected observation here was that the wash itself caused a small and transient increase in NFAT-NF (open circles in Fig.6). This likely reflects the effect of mechanical stimulation on cytoplasmic Ca^{2+} concentration and prevents meaningful comparison of information transfer during and beyond the first GnRH pulse. Nevertheless, we were able to calculate the additional information due to sensing both pulses (~0.1 Bit) and the MI between responses in pulse 2 and 1 (~1.0 Bit). Accordingly, the wet-lab data parallel the situation simulated in Fig.5 with high effector stability, implying that the sources of cell-cell heterogeneity are relatively stable over time so that there is little additional information to be gained from sensing the second pulse, at least in this time-frame and under our experimental conditions.

DISCUSSION

Information theory-derived statistical measures, such as the MI between a stimulus and a response, can be used to quantify information transfer via cell signaling pathways, taking into account both the dynamic range and the cell-cell variability of responses. Importantly, MI can be measured without knowledge of the transduction mechanism, and MI values are unaffected by non-linear transformations of the signal or response so they are not influenced by non-linear input-output relationships prevalent in cell signaling pathways (1). Here we have use this approach to estimate information transfer via GnRHR to ERK and to NFAT, placing emphasis on the relevance of dynamics for GnRH sensing. For each effector we found that most of the information available from the environment was lost through signaling (i.e. that with 3 Bits of information available, <1 Bit was transferred) and that although information transfer could be increased by joint sensing (of both effectors) and by trajectory sensing, the additional information we observed was small. We also developed a hybrid mechanist/probabilistic model of GnRH signaling to NFAT and used this to simulate responses to constant or pulsatile GnRH. The model predicts that a second pulse of GnRH will provide considerable additional information when cell-cell variability reflects rapidly changing effector levels but not when it is due to variation in effectors that is stable over the time-frame of the repeated pulses. Live cell imaging experiments closely paralleled the latter scenario, yielding very little additional information from a second GnRH pulse. To our knowledge, this is the first study addressing the information gain from repeat hormone stimulation, and in general, it reveals that the additional information available from sensing repeat pulses depends on stability of network componentry.

The work described here extends a recent study in which we used the same information theoretic approach to quantify information transfer via GnRHR to ERK in HeLa cells transduced for expression of GnRHR (9). This revealed MI values (I(ppERK;GnRH) of <1 Bit which implies that the individual cells cannot unambiguously distinguish between even two states of the environment (i.e. two GnRH concentrations). This is consistent with information transfer estimates for other receptors and/or effectors (2-4,7) but is still somewhat surprising, as it is well known that GnRH elicits graded signaling, gene expression and gonadotropin secretion over broad concentration ranges in many models (13,14,20-23). In the previous study we considered the possibility that I(ppERK;GnRH) values of <1 Bit might reflect negative feedback as it is well established that ERK responses are shaped by multiple feedback pathways (32,34-36). We found that ERK-mediated negative feedback could reduce information transfer by reducing response amplitude, but could also increase it by reducing cell-cell variability. Thus, information transfer was maximal with intermediate feedback but nevertheless, was always <1 Bit. Another possible explanation for these low MI values is that little information is transferred via GnRHR to ERK because with this bifurcating signaling system, most information actually passes via the IP_3/Ca^{2+}/calmodulin pathway. Alternatively, information transfer could have been underestimated by use of a heterologous receptor expression system, or by simply missing the optimal time-point for its measurement. However, the data herein argue against each of these possibilities. Notably, the fixed cell experiments (Figs.1,2 and Supplemental Figs.1,2) reveal that information transfer to NFAT is actually lower than to ERK at most time-points, that information transfer is comparable for heterologously expressed GnRHR in HeLa cells and for endogenous GnRHR of LβT2 cells, and that for all experimental readouts and both models, MI values were <1 at all time points considered. Another possibility is that GnRH sensing is underestimated by consideration of a single pathway or effector because simultaneous activation of multiple effectors improves it. To address this we imaged ERK and NFAT responses in identical cells in order to calculate joint MI (Fig.2 and Supplemental Fig.2). This revealed that for both cellular models and for both upstream activation readouts (ppERK and NFAT-NF measures) and downstream transcriptional readouts (Egr1-driven zsGREEN and NFAT-RE-driven asRED expression) joint MI values were always greater than for either measure alone. However, the increase was relatively small (often <0.1 Bit). Thus, the current study confirms the previous observation that most information about GnRH concentration is lost through signaling and importantly, extends it by showing that I(response;GnRH) values are <1 Bit over full time courses with endogenous GnRHR and for each of the responses considered, alone and in combination.

A particularly interesting observation here is that I(ppERK;GnRH), I(NFAT-NF;GnRH) and joint MI values showed different time-dependencies. This was most obvious in HeLa cells (Supplemental Fig.2C) where I(ppERK;GnRH) dropped from 0.64 to 0.09 Bits from 5 to 60 min whereas I(NFAT-NF;GnRH) remained unaltered (at approximately 0.45 Bits) and joint MI showed only a small reduction (from 0.73 to 0.53) over the same period. Recent work on growth factor stimulated signaling (7) revealed how concomitant activation of distinct pathways made information transfer robust to pharmacological manipulation because compensation occurred (i.e. where one pathway was inhibited but information transfer through another was retained). Our data reveal a related situation where concomitant activation of two pathways makes information transfer robust to the reduction in sensing due to adaptation in one of them over time. Here, it is important to recognise that this robustness, in terms of information transfer, does not equate to biological redundancy. Consider the situation where an extracellular stimulus elicits single cell ERK and NFAT responses that are perfectly correlated with one-another, yet ERK and NFAT mediate different responses by activation of different effectors. In this scenario, ablation of ERK would not reduce the information the cell has about hormone concentration in its environment but would abrogate the ERK-mediated response. Similarly, ablation of NFAT would not reduce the information the cell has about hormone concentration in its environment but would abrogate the NFAT-mediated response. Thus, in this bifurcating signaling system, the observed robustness in information transfer from receptor to ERK and NFAT tells us nothing about information transfer downstream of ERK and NFAT.

Together the data outlined above reveal that GnRH-responsive cells gain more information by sensing both ERK and NFAT pathways, but that this additional information is rather modest, and the concomitant activation of both pathways may serve instead to ensure robust information transfer. However, they still do not explain the relatively low I(response;GnRH) values obtained so we also considered the possibility that single time-point measures greatly underestimate information transfer. Indeed, the time-courses in Fig.2 reveal I(ppERK;GnRH) and I (NFAT-NF;GnRH) values at 60 min to be higher than those at 240 min but this clearly does not mean that the cells had obtained less information over 240 min than they had over 60 min. Instead, it shows that the 240 min snap-shot underestimates the amount of information transferred. We recently argued on the basis of transcriptional readouts for GnRHR signaling to ERK, that cells must gain additional information by sensing response trajectory (9) and here we have taken a more direct approach, using live cell imaging of NFAT1c-EFP translocation responses and cell tracking. This enabled us to calculate MI values not only using snap-shots of individual cell responses at specific time-points, but also using single cell integrated responses or response trajectories. In the first instance we simply stimulated GnRHR-expressing HeLa cells for 60 min with GnRH (0 or 10^{-11}-10^{-9}M) and consistent with the fixed cell experiments, this revealed I(NFAT-NF;GnRH) values of approximately 0.5 Bits at all time points (Fig 4). MI values were higher for the integrated readout and when trajectory was considered but the increase was small (<0.1 Bits) so little or no additional information was gained by sensing the NFAT translocation response trajectory. However, GnRH is secreted in pulses so we were particularly interested in this scenario, and explored it theoretically by developing a hybrid (deterministic/stochastic) model of the GnRH signaling pathway (from GnRHR to NFAT). We introduced heterogeneity in the expression levels of the receptor and calmodulin, and simulations revealed the potential for additional information to be gained by sensing beyond the GnRH pulse (Fig.5), as well as by sensing a second GnRH pulse (Fig.6). Since cell-cell variability could reflect stable differences in system componentry or alternatively, differences that are either random or rapidly changing over time we considered both possibilities by varying the timescale at which the total amount of GnRHR and calmodulin fluctuate. Model simulations suggested that sensing the second GnRH pulse would provide little or no additional information if the effectors were stable (such that responses in one pulse were predictive of responses in the other) and the data from dual pulse live-cell imaging experiments were consistent with this scenario. However, since the additional information is related to the reliability with which responses in one pulse predict those in the other, we would anticipate that the information gained from a second pulse would be increased by increasing the time between the pulses. More generally, if we consider two brief pulses of stimulus and a system where cell-cell variability reflects the concentration of effectors, the additional information gained from the second pulse will increase as inter-pulse interval increases and will decrease as effector stability increases.

The data described also relate to the more general question of why pulsatile signals are so prevalent in biological systems. We have recently explored this by deterministic modelling of pulsatile stimulation with varied pulse width, amplitude and frequency (31). This revealed how pulsatility can increase signaling efficiency in the sense that with pulsatile and constant stimuli and identical input integrals, the system output can be much greater with the pulsatile stimulation. This occurs largely because signaling continues in the intervals between the pulse and the extent of this depends on activation and inactivation rates that will differ for different effectors. Consequently, with pulsatile stimuli input-output relationships for different effectors are not superimposable, and this can give output-specific frequency-response relationships where no such specificity occurs with concentration-response relationships (31). Here, we consider a third possibility, that with pulsatility there is a substantial information gain from repeated stimuli, but our data argue against this, at least for GnRH stimulation in the experimental paradigms considered. Another important general observation here is that, even when joint sensing or trajectory are considered, our I(response;GnRH) values were always <1. Thus the individual GnRH-responsive cells cannot distinguish between even two GnRH concentrations, and this contrasts to numerous published studies showing dose-dependent effects of GnRH on populations of GnRH-responsive cells (including the examples herein). Clearly cell populations can discern GnRH concentrations more effectively than individual cells, and this could reflect averaging of responses over multiple cells and/or cell-cell communication providing additional information. The latter possibility is of particular interest as gonadotropes communicate with one-another via gap junctions (37,38), and such communication could improve sensing. Thus, although it is individual cells that have to sense and respond to GnRH in their environment, these decisions could well be informed by additional information from their neighbours.

In summary, we have used single cell measures to quantify GnRHR-mediated information transfer to ERK and NFAT and find that signaling is inefficient, in the sense that most information about GnRH concentration in the environment is lost through signaling. Information transfer was increased by joint sensing of both pathways but the additional information was small and little or no additional information was gained by sensing individual cell NFAT response trajectories over time. Since GnRH secretion is pulsatile we also explored the sensing of input dynamics by developing a model of GnRH signaling that suggests, for NFAT signaling at least, that cells gain as much information by sensing beyond the GnRH pulse as they do during it. These simulations also highlight the importance of effector stability because when cell-cell variability reflects differences in rapidly fluctuating effector levels, additional information is predicted to be gained by sensing two GnRH pulses. In contrast, where there is comparable cell-cell variability in slowly fluctuating effector levels, responses in one pulse are predictive of those in another so there is little additional information to be gained by sensing both. Parallel wet-lab experiments suggest that the latter scenario holds true for GnRH signaling via the PLC/ Ca^{2+}/calmodulin/calcineurin/NFAT pathway, that (within the time-frames considered) cell-cell variability is low so that response trajectories are reproducible from pulse to pulse. Thus although the pulsatile input can increase signaling efficiency and specificity (31), these first information theoretic studies of dynamic GnRH sensing suggest that the amount of information the cell has about GnRH concentration in its environment is not greatly increased by sensing additional pulses.

The abbreviations used are: GnRH, gonadotropin-releasing hormone; GnRHR, GnRH receptor; PKC, protein kinase C; EFP, emerald green fluorescent protein; ERK, extracellular signal-regulated kinase (we use the term ERK to mean ERK1 and/or ERK2); ppERK, dual phosphorylated (activated) ERK; NFAT, nuclear-factor of activated T-cells; GPCR, G-protein coupled receptor; Ad, adenovirus; FCS, fetal calf serum; DMEM, Dulbecco's modified Eagle's medium; DAPI, 4'-6-Diamidino-2-phenylindole; MI, mutual information; FL, fluctuation lifetime; CaM, calmodulin; NF, nuclear fraction; AFU, arbitrary fluorescence units; AUC, area under the curve; TNF, tumour necrosis factor; NGF, nerve growth factor; PACAP, pituitary adenylyl cyclase-activating polypeptide; CREB, cyclic AMP response element binding protein.

Address for correspondence and reprint requests: Prof. Craig A McArdle, Laboratories for Integrative Neuroscience and Endocrinology, School of Clinical Sciences, University of Bristol, Bristol, BS13NY, UK. Tel: 0044 117 3313077. e-mail:craig.mcardle@bristol.ac.uk

Supported by a Biochemical and Biophysical Science Research Council award to CAM and KT-A (BBSRC BB/J014699/1). MV acknowledges the support of MRC (Strategic Skills Development Fellowship in Biomedical Informatics) and EPSRC via grant number EP/N014391/1.

Disclosure Statement; The authors have nothing to disclose.

REFERENCES

1. Bowsher CG, Swain PS. Environmental sensing, information transfer, and cellular decision-making. Curr Opin Biotechnol 2014; 28:149-155
2. Cheong R, Rhee A, Wang CJ, Nemenman I, Levchenko A. Information transduction capacity of noisy biochemical signaling networks. Science 2011; 334:354-358
3. Brennan MD, Cheong R, Levchenko A. Systems biology. How information theory handles cell signaling and uncertainty. Science 2012; 338:334-335
4. Voliotis M, Perrett RM, McWilliams C, McArdle CA, Bowsher CG. Information transfer by leaky, heterogeneous, protein kinase signaling systems. Proceedings of the National Academy of Sciences of the United States of America 2014; 111:E326-333
5. Voliotis M, Bowsher CG. The magnitude and colour of noise in genetic negative feedback systems. Nucleic acids research 2012; 40:7084-7095
6. Bowsher CG, Voliotis M, Swain PS. The fidelity of dynamic signaling by noisy biomolecular networks. PLoS computational biology 2013; 9:e1002965
7. Uda S, Saito TH, Kudo T, Kokaji T, Tsuchiya T, Kubota H, Komori Y, Ozaki Y, Kuroda S. Robustness and compensation of information transmission of signaling pathways. Science 2013; 341:558-561
8. Selimkhanov J, Taylor B, Yao J, Pilko A, Albeck J, Hoffmann A, Tsimring L, Wollman R. Systems biology. Accurate information transmission through dynamic biochemical signaling networks. Science 2014; 346:1370-1373
9. Garner KL, Perrett RM, Voliotis M, Bowsher C, Pope GR, Pham T, Caunt CJ, Tsaneva-Atanasova K, McArdle CA. Information Transfer in Gonadotropin-releasing Hormone (GnRH) Signaling: EXTRACELLULAR SIGNAL-REGULATED KINASE (ERK)-MEDIATED FEEDBACK LOOPS CONTROL HORMONE SENSING. The Journal of biological chemistry 2016; 291:2246-2259
10. McArdle CA, Forrest-Owen W, Willars G, Davidson J, Poch A, Kratzmeier M. Desensitization of gonadotropin-releasing hormone action in the gonadotrope-derived alpha T3-1 cell line. Endocrinology 1995; 136:4864-4871
11. Armstrong SP, Caunt CJ, Fowkes RC, Tsaneva-Atanasova K, McArdle CA. Pulsatile and sustained gonadotropin-releasing hormone (GnRH) receptor signaling: does the Ca2+/NFAT signaling pathway decode GnRH pulse frequency? The Journal of biological chemistry 2009; 284:35746-35757
12. Caunt CJ, Finch AR, Sedgley KR, McArdle CA. Seven-transmembrane receptor signalling and ERK compartmentalization. Trends in endocrinology and metabolism: TEM 2006; 17:276-283
13. Naor Z. Signaling by G-protein-coupled receptor (GPCR): studies on the GnRH receptor. Frontiers in neuroendocrinology 2009; 30:10-29
14. Millar RP, Lu ZL, Pawson AJ, Flanagan CA, Morgan K, Maudsley SR. Gonadotropin-releasing hormone receptors. Endocrine reviews 2004; 25:235-275
15. Caunt CJ, Finch AR, Sedgley KR, McArdle CA. GnRH receptor signalling to ERK: kinetics and compartmentalization. Trends in endocrinology and metabolism: TEM 2006; 17:308-313
16. Bliss SP, Miller A, Navratil AM, Xie J, McDonough SP, Fisher PJ, Landreth GE, Roberson MS. ERK signaling in the pituitary is required for female but not male fertility. Mol Endocrinol 2009; 23:1092-1101

17. Armstrong SP, Caunt CJ, McArdle CA. Gonadotropin-releasing hormone and protein kinase C signaling to ERK: spatiotemporal regulation of ERK by docking domains and dual-specificity phosphatases. Mol Endocrinol 2009; 23:510-519
18. Armstrong SP, Caunt CJ, Fowkes RC, Tsaneva-Atanasova K, McArdle CA. Pulsatile and sustained gonadotropin-releasing hormone (GnRH) receptor signaling: does the ERK signaling pathway decode GnRH pulse frequency? The Journal of biological chemistry 2010; 285:24360-24371
19. Lewis CE, Richards PS, Morris JF. Heterogeneity of responses to LH-releasing hormone and phorbol ester among rat gonadotrophs: a study using a reverse haemolytic plaque assay for LH. Journal of molecular endocrinology 1989; 2:55-63
20. Stojilkovic SS, Catt KJ. Novel aspects of GnRH-induced intracellular signaling and secretion in pituitary gonadotrophs. Journal of neuroendocrinology 1995; 7:739-757
21. McArdle CA, Bunting R, Mason WT. Dynamic video imaging of cystolic Ca(2+) in the alphaT3-1, gonadotrope-derived cell line. Molecular and cellular neurosciences 1992; 3:124-132
22. Ruf F, Park MJ, Hayot F, Lin G, Roysam B, Ge Y, Sealfon SC. Mixed analog/digital gonadotrope biosynthetic response to gonadotropin-releasing hormone. The Journal of biological chemistry 2006; 281:30967-30978
23. Ruf F, Hayot F, Park MJ, Ge Y, Lin G, Roysam B, Sealfon SC. Noise propagation and scaling in regulation of gonadotrope biosynthesis. Biophysical journal 2007; 93:4474-4480
24. Caunt CJ, Perett RM, Fowkes RC, McArdle CA. Mechanisms of GnRH-induced extracellular signal-regulated kinase nuclear localization. PloS one 2012; 7:e40077
25. Perrett RM, Fowkes RC, Caunt CJ, Tsaneva-Atanasova K, Bowsher CG, McArdle CA. Signaling to extracellular signal-regulated kinase from ErbB1 kinase and protein kinase C: feedback, heterogeneity, and gating. The Journal of biological chemistry 2013; 288:21001-21014
26. Caunt CJ, Armstrong SP, Rivers CA, Norman MR, McArdle CA. Spatiotemporal regulation of ERK2 by dual specificity phosphatases. The Journal of biological chemistry 2008; 283:26612-26623
27. Caunt CJ, Rivers CA, Conway-Campbell BL, Norman MR, McArdle CA. Epidermal growth factor receptor and protein kinase C signaling to ERK2: spatiotemporal regulation of ERK2 by dual specificity phosphatases. The Journal of biological chemistry 2008; 283:6241-6252
28. Caunt CJ, McArdle CA. Stimulus-induced uncoupling of extracellular signal-regulated kinase phosphorylation from nuclear localization is dependent on docking domain interactions. Journal of cell science 2010; 123:4310-4320
29. Hislop JN, Everest HM, Flynn A, Harding T, Uney JB, Troskie BE, Millar RP, McArdle CA. Differential internalization of mammalian and non-mammalian gonadotropin-releasing hormone receptors. Uncoupling of dynamin-dependent internalization from mitogen-activated protein kinase signaling. The Journal of biological chemistry 2001; 276:39685-39694
30. I. Nemenman, F. Shafee, and W. Bialek. Entropy and inference, revisited. In TG Dietterich, S Becker, and Z Ghahramani, editors, Advances in Neural Information Processing Systems 14, Cambridge, MA, 2002. MIT Press.
31. Pratap A, Garner KL, Voliotis M, Tsaneva-Atanasova K, McArdle CA. Mathematical modeling of gonadotropin-releasing hormone signaling. Molecular and cellular endocrinology 2016;
32. Santos SD, Verveer PJ, Bastiaens PI. Growth factor-induced MAPK network topology shapes Erk response determining PC-12 cell fate. Nature cell biology 2007; 9:324-330

33. Perrett RM, Voliotis M, Armstrong SP, Fowkes RC, Pope GR, Tsaneva-Atanasova K, McArdle CA. Pulsatile Hormonal Signaling to Extracellular Signal-Regulated Kinase: Exploring System Sensitivity to Gonadotropin-Releasing Hormone Pulse Frequency and Width. The Journal of biological chemistry 2014;
34. Kholodenko BN, Hancock JF, Kolch W. Signalling ballet in space and time. Nature reviews Molecular cell biology 2010; 11:414-426
35. Caunt CJ, Sale MJ, Smith PD, Cook SJ. MEK1 and MEK2 inhibitors and cancer therapy: the long and winding road. Nature reviews Cancer 2015; 15:577-592
36. Shankaran H, Wiley HS. Oscillatory dynamics of the extracellular signal-regulated kinase pathway. Current opinion in genetics & development 2010; 20:650-655
37. McArdle CA, Roberson MS. Gonadotropes and Gonadotropin-Releasing Hormone Signaling in “Knobil and Neill’s Physiology of Reproduction” 4th Edition. Ed. Plant TM and Zeleznick AJ. 2015. Pub: Elsevier. Volume 1, Chapter, 10 pp 335-397
38. Denef C. Paracrinicity: the story of 30 years of cellular pituitary crosstalk. Journal of neuroendocrinology 2008; 20:1-70

Figure 1. Quantifying Information transfer via GnRHR to ERK and NFAT in LβT2 cells. Panel A: LβT2 cells in 96 well plates were continuously stimulated for varied periods with 0 or 10^{-12}-10^{-6}M GnRH as indicated and then fixed and stained (DAPI and ppERK) before image capture and analysis. The data shown are population-averaged nuclear ppERK measures in arbitrary fluorescence units (AFU) and are means ± SEMs from 3 separate experiments, each with triplicate wells (n=3). Background values (without fluorophore) were 120-150 AFU and were not subtracted. Log EC_{50} values were -9.03 ± 0.39, -8.07 ± 0.16, -7.95 ± 0.19, -8.01 ± 0.53, -7.76 ± 0.60 and -7.34 ± 0.74 at 5, 15, 30, 60, 120 and 240 min, respectively. One way ANOVA revealed time to be a significant variable (P<0.05) and post-hoc Bonferroni tests (comparing to the 5 min data) revealed a significant difference at 240 min (P<0.05) but not at any other time point. Panel B: The single cell ppERK measures from the full concentration response curves in A were used to calculate the MI between GnRH concentration and ppERK at each time-point and these I(ppERK;GnRH) values (in Bits) are plotted against time. Panel C: Ad NFAT-EFP transduced LβT2 cells in 96 well plates were stimulated for varied periods with 0 or 10^{-12}-10^{-6}M GnRH as indicated and then fixed and stained (DAPI) before image capture and analysis. NFAT-EFP fluorescence intensity was determined for the nucleus and cytoplasm and used (after subtraction of background values which were ~200 AFU) to calculate the proportion of NFAT-EFP in the nucleus. The data shown are population-averaged measures of this NFAT-nuclear fraction (NFAT-NF) and are means ± SEMs from 3 separate experiments, each with triplicate wells (n=3). Panel D: The single cell NFAT-NF measures from the full concentration response curves in C were used to calculate the MI between GnRH concentration and NFAT-NF and these I(NFAT-NF;GnRH) values (in Bits) are plotted against time. The data in A and C are replotted against time in Supplemental Fig.1 to better illustrate response kinetics.

Figure 2. Joint sensing of ERK and NFAT signaling in LβT2 cells. For panels A-C, LβT2 cells transduced with Ad NFAT-EFP were continuously stimulated 5, 20 or 60 min with 0 or 10^{-12}–10^{-6}M GnRH as indicated before being fixed, stained (DAPI and ppERK) and imaged for ppERK and NFAT-NF as described under Fig.1, except that in this case both were measured in identical cells. The single cell data from the full concentration response curves were then used to calculate MI between GnRH concentration and each response (ppERK or NFAT-NF) and also the joint MI between GnRH and both responses (Joint). For panels D-E, LβT2 cells transduced

with Ad Egr1-zsGREEN and Ad NFAT RE-asRED were stimulated for 4, 6 or 8 hr with 0 or 10^{-12}–10^{-6}M GnRH as indicated before being fixed, stained (DAPI) and imaged to quantify zsGREEN and asRED. The single cell data were then used to calculate MI between GnRH and the expression level for each reporter and also the joint MI between GnRH and both reporters (Joint). The data shown are means ± SEM (n=5-7) for population averaged measures of ppERK (A), NFAT translocation (NFAT-NF, B), Egr1-driven zsGREEN expression (D) and NFAT RE-driven asRED expression (E), as well as I(response;GnRH) (C and F) in Bits. Log EC_{50} values for panel A were -8.24±0.07, -8.01±0.08 and -7.76±0.16 (n=7) at 5, 20 and 60 min, respectively and one way ANOVA revealed that time was not a significant source of variation (P>0.05).

Figure 3. Sensing Dynamics and Live Cell NFAT-EFP Imaging. HeLa cells transduced with Ad GnRHR and Ad NFAT-EFP were stained with Hoechst dye (for imaging of nuclei) transferred to live cell imaging medium and imaged at 37^{o}C both before and during continuous stimulation with 0, 10^{-11}, 10^{-9} or 10^{-7}M GnRH. Automated image analysis algorithms were used to calculate the nuclear fraction of NFAT-EFP (NFAT-NF, calculated for each cell and at each time-point) and individual cells were tracked over time. The individual cell time-course were then inspected for removal of cells in which tracking had failed or had time 0 NFAT-NF values <0.4 or >0.55 (this removed <10% of cells as outliers). Panels A and B show responses of representative individual cells stimulated with 10^{-9}M GnRH and selected to illustrate distinct response patterns; little or no response (grey shade traces in A), rapid and sustained increases (red shade traces in A), rapid but not sustained (blue shade traces in B) and delayed (red traces in B). Most cells (>50-75%) showed rapid and sustained responses and very few showed delayed responses (3/166 for this data set). Population averaged responses for all tracked cells are shown in panel C) (mean±SEM, n=72-167). I(NFAT-NF;GnRH) values for the tracked cells were calculated for each individual time-point and are shown in panel D (mean±SD). I(NFAT-NF;GnRH) values were also calculated from the same tracked cells using the area under the curve (AUC) over the full 60 min as the response, and also using 3 time-points to taking individual cell response trajectories into account as described in Materials and Methods. These values are also shown (along with the maximum snap-shot value) in panel D.

Figure 4. Mixed Mechanistic and Probabilistic Modelling of NFAT Responses to GnRH Pulses: Sensing During and Beyond the GnRH Pulse. We adapted a deterministic model of GnRH signaling (31) and used it to simulate responses during and immediately after a 15 min pulse of 0, 10^{-11}, 10^{-9} and 10^{-7} M GnRH. We introduced heterogeneity into the concentration of two effectors, the GnRHR and calmodulin (CaM, which equates to M in (31)). For each of these we added synthesis and degradation to the model and introduced cell-cell variability by allowing them to fluctuate, simulating unstable effector expression with a fluctuation lifetime (FL) of 10 and stable effector expression with an FL of 10000. Panels A shows population averaged data for simulations with 10^{-7}M GnRH with unstable (left panels) or stable (right panels) effector expression (means±SEM, n=1000) and panels B show representative traces for 25 individual cells. The GnRHR and CaM concentrations for the same representative cells are shown in panels C and D. The individual cell simulation data were used to calculate MI using (as response) either the 15 min snap-shot data or the AUCs during the 15 min GnRH pulse or the following 15 min. The bar charts show these MI values (means±SD) for the unstable and stable scenarios (left and right panels, respectively) along with the additional information gained by sensing both during and beyond the pulse, calculated as described in the Materials and Methods. Note that information transfer during and beyond the pulse are comparable to one-another (and to the snap-

shot values) and that there is little information gained by sensing both, particularly when effector expression is stable.

Figure 5. Mixed Mechanistic and Probabilistic Modelling of NFAT Responses to GnRH Pulses: Sensing Two Pulses. The data in Fig.5 are from a larger series of simulations in which we considered 4 effector stabilities, and also followed the first 15 min GnRH pulse with a 120 min interval and then a second pulse (30 min, at the same GnRH concentration as the first) so that we could calculate not only information transfer during each pulse but also the additional information gained by sensing both. Again, we ran simulations for 1000 cells at each GnRH concentration/effector stability combination. Panel A shows population averaged data for simulations with 10^{-7}M GnRH at each of four stability's (FL 10, 100, 1000 and 10000, means ± SEM, n=1000) and panels B show representative traces for 25 individual cells. Panel C shows MI between GnRH and the predicted NFAT-NF response using AUCs for pulse 1 or pulse 2, panel D shows the additional information gained by sensing both pulses and panel E shows MI between responses in pulse 1 and 2. Panels C-E are plotted against FL (where $\log_{10}$ FL values of 1 and 4 represent the most unstable and stable scenario, respectively) and show means ±SD. Note that at any given time point, mean values and variance are comparable for NFAT-NF (A) as well as for , GnRHR and CaM (not shown), but as effector stability is increased this increases MI between the pulse 1 and pulse 2 responses (E), and reduces additional information gained from the 2 second pulse (D).

Figure 6. Sensing Dynamics With Repeated Stimulation and Live Cell NFAT-EFP Imaging. Panel A: HeLa cells transduced with Ad GnRHR and Ad NFAT-EFP were stained with Hoechst dye transferred to live cell imaging medium and imaged at 37°C both before and during stimulation with 0, 10^{-11}, 10^{-9} or 10^{-7}M GnRH for 15 min (first grey bar). The plate was then removed from the stage, cells were washed (with PBS, 3 times over 5 min) and the plate was returned to the stage. The cells were imaged for a further 2 hr before repeat stimulation (second grey bar) for 60 min using the same concentrations of GnRH. Image analysis and data processing were as described under Fig.4. The data shown are pooled from the tracked cells in 3 repeated experiments (mean ± SEM, n = 67-489). Panel B: MI values calculated using the AUC for the first 15 min of stimulation with GnRH in pulse 1 or pulse 2, the additional information gained by sensing both and the MI between responses in pulse 1 and pulse 2. Note that these data are consistent with the stable-effector scenario of Fig.5, with little additional information gained by sensing both pulses because responses in one pulse are highly predictive of those in the other.

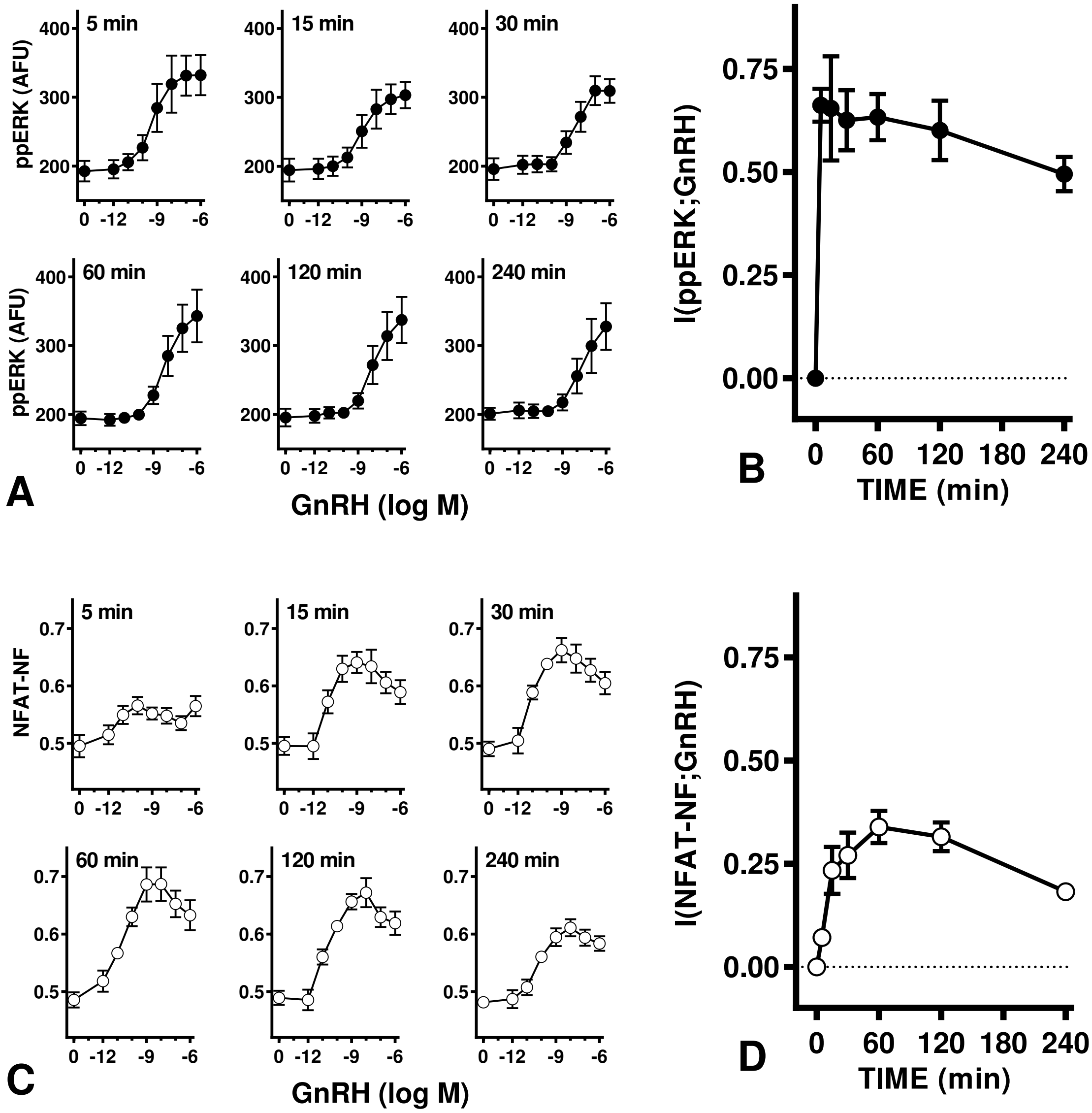
A
ppERK (AFU)
5 min
15 min
30 min
60 min
120 min
240 min
GnRH (log M)
B
I(ppERK;GnRH)
TIME (min)
C
NFAT-NF
D
I(NFAT-NF;GnRH)
TIME (min)

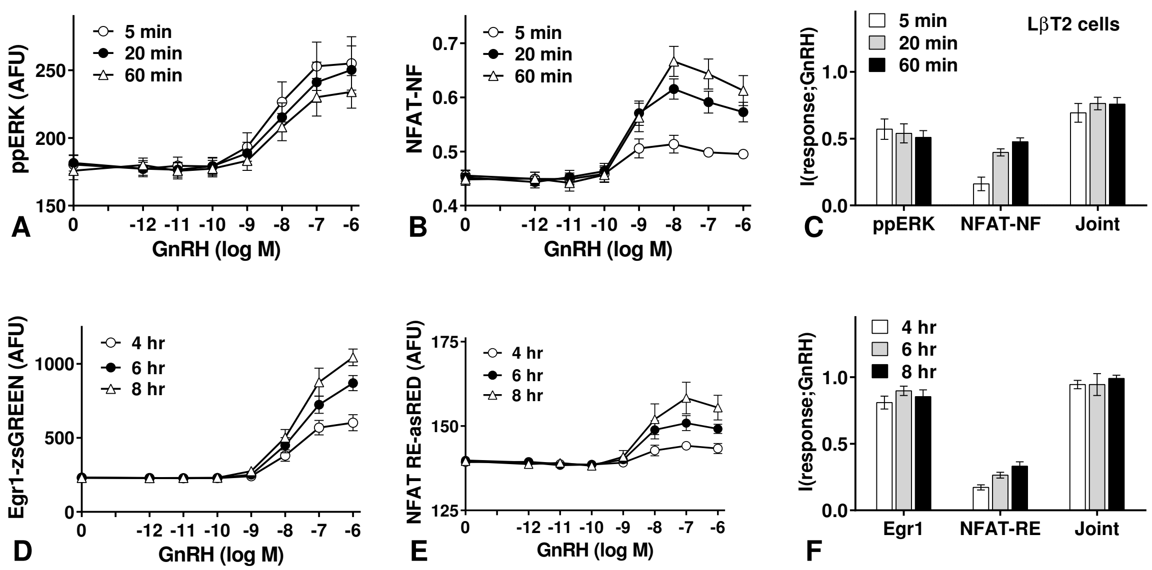
ppERK (AFU)
5 min
20 min
60 min
GnRH (log M)
A
NFAT-NF
B
I(response;GnRH)
LβT2 cells
ppERK
NFAT-NF
Joint
C
Egr1-zsGREEN (AFU)
4 hr
6 hr
8 hr
D
NFAT RE-asRED (AFU)
E
Egr1
NFAT-RE
F

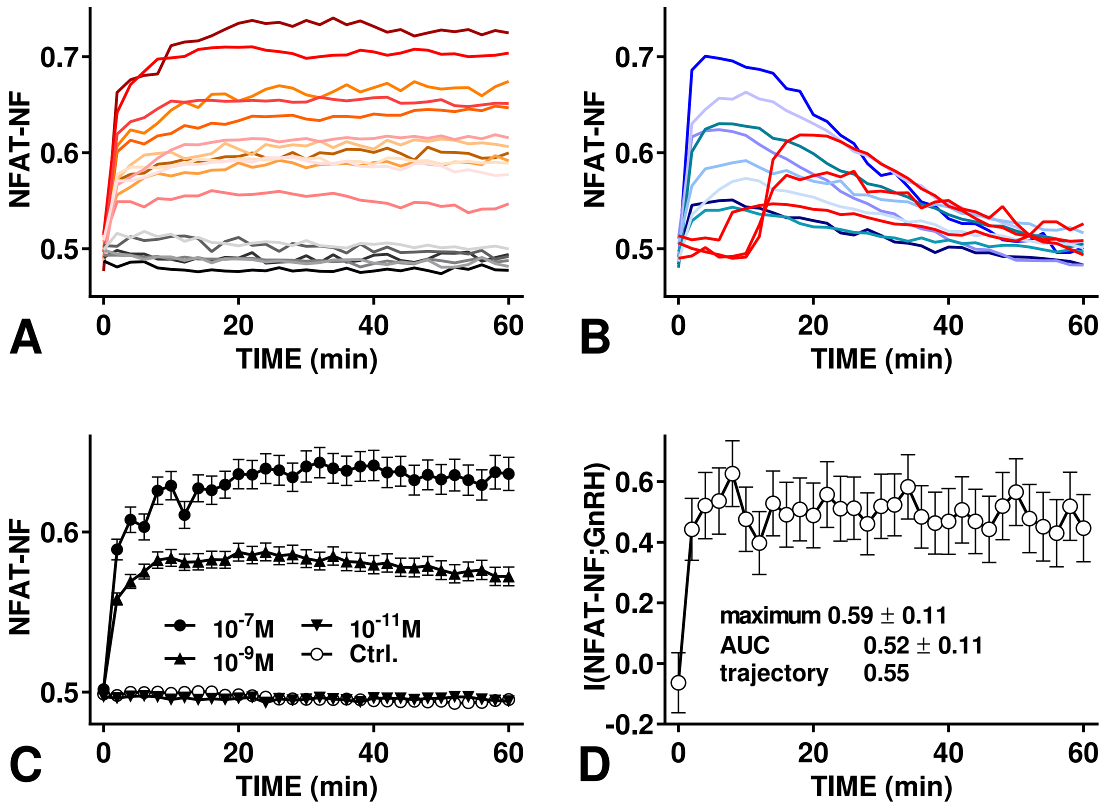

A
B
C
D
NFAT-NF
TIME (min)
I(NFAT-NF;GnRH)
10^{-7}M
10^{-9}M
10^{-11}M
Ctrl.
maximum 0.59 ± 0.11
AUC 0.52 ± 0.11
trajectory 0.55

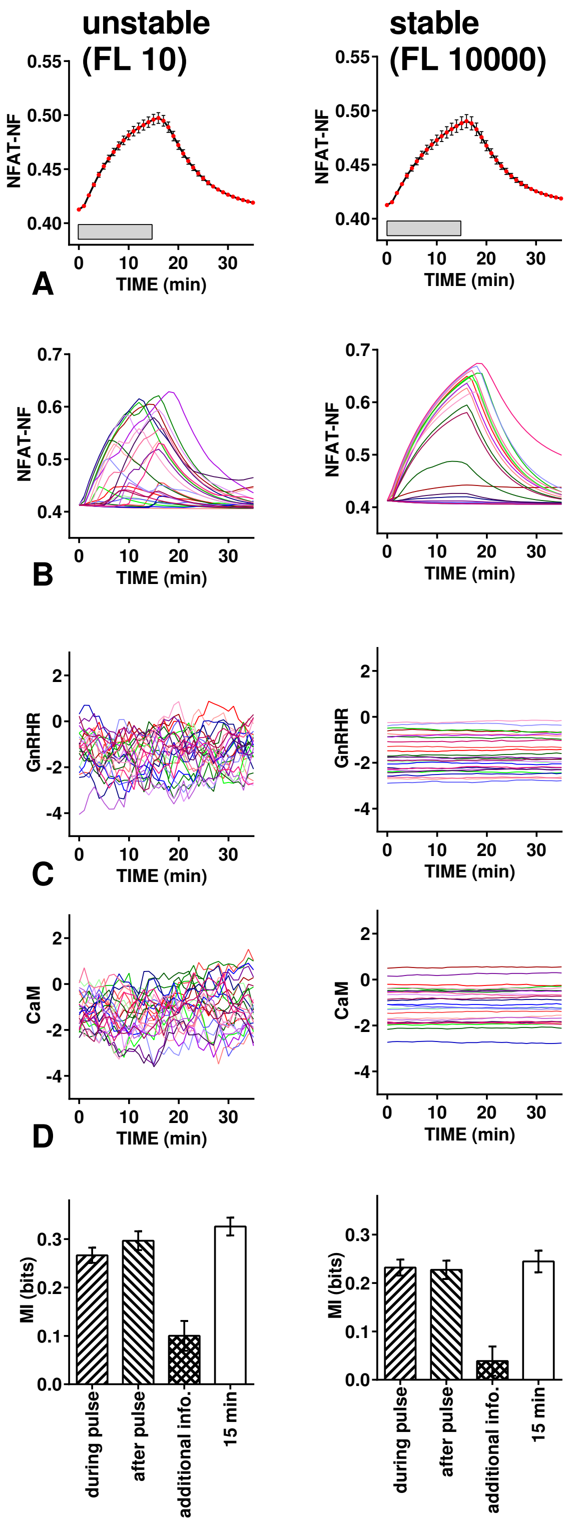
unstable
(FL 10)
stable
(FL 10000)
NFAT-NF
0.55
0.50
0.45
0.40
0
10
20
30
TIME (min)
A
NFAT-NF
0.7
0.6
0.5
0.4
B
GnRHR
2
0
-2
-4
C
CaM
D
MI (bits)
0.3
0.2
0.1
0.0
during pulse
after pulse
additional info.
15 min

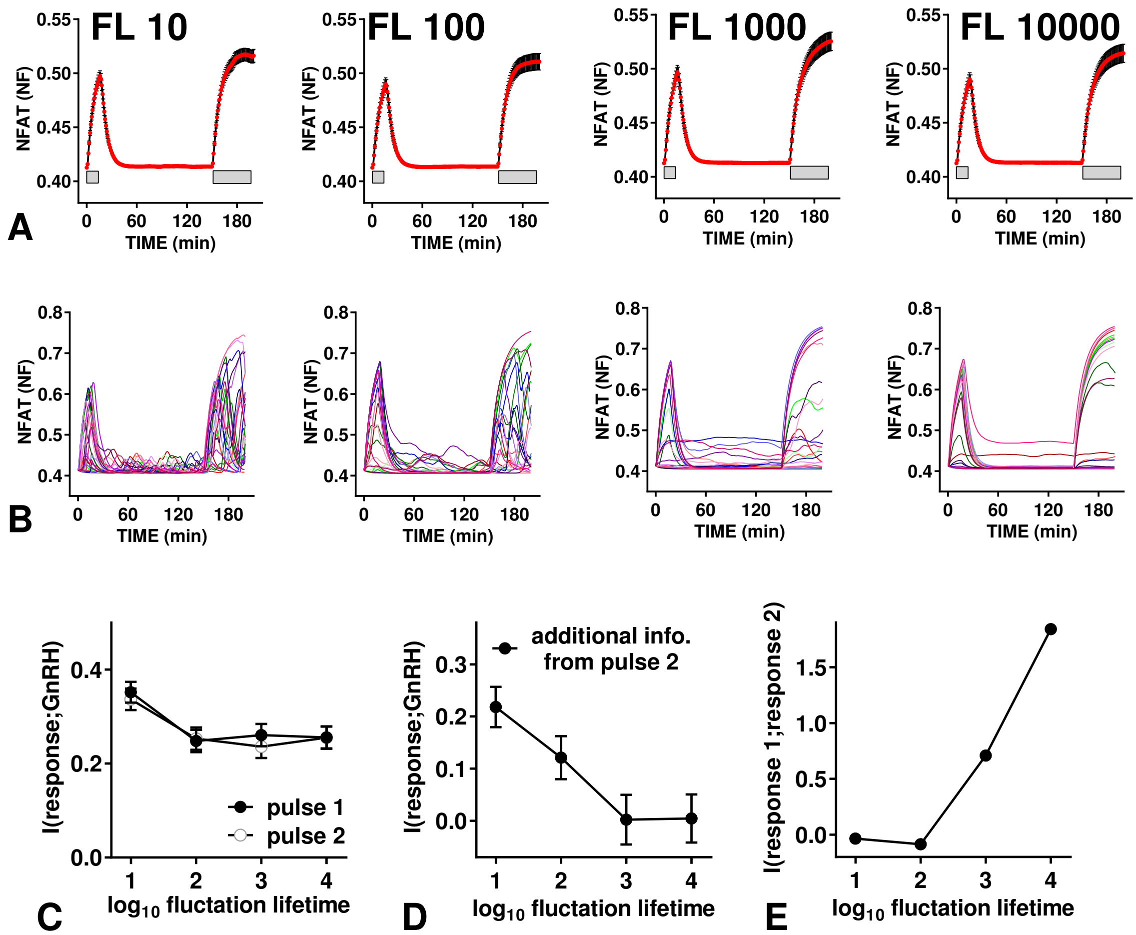
FL 10
FL 100
FL 1000
FL 10000
NFAT (NF)
TIME (min)
A
B
C
D
E
I(response;GnRH)
pulse 1
pulse 2
log10 fluctation lifetime
additional info.
from pulse 2
I(response 1;response 2)

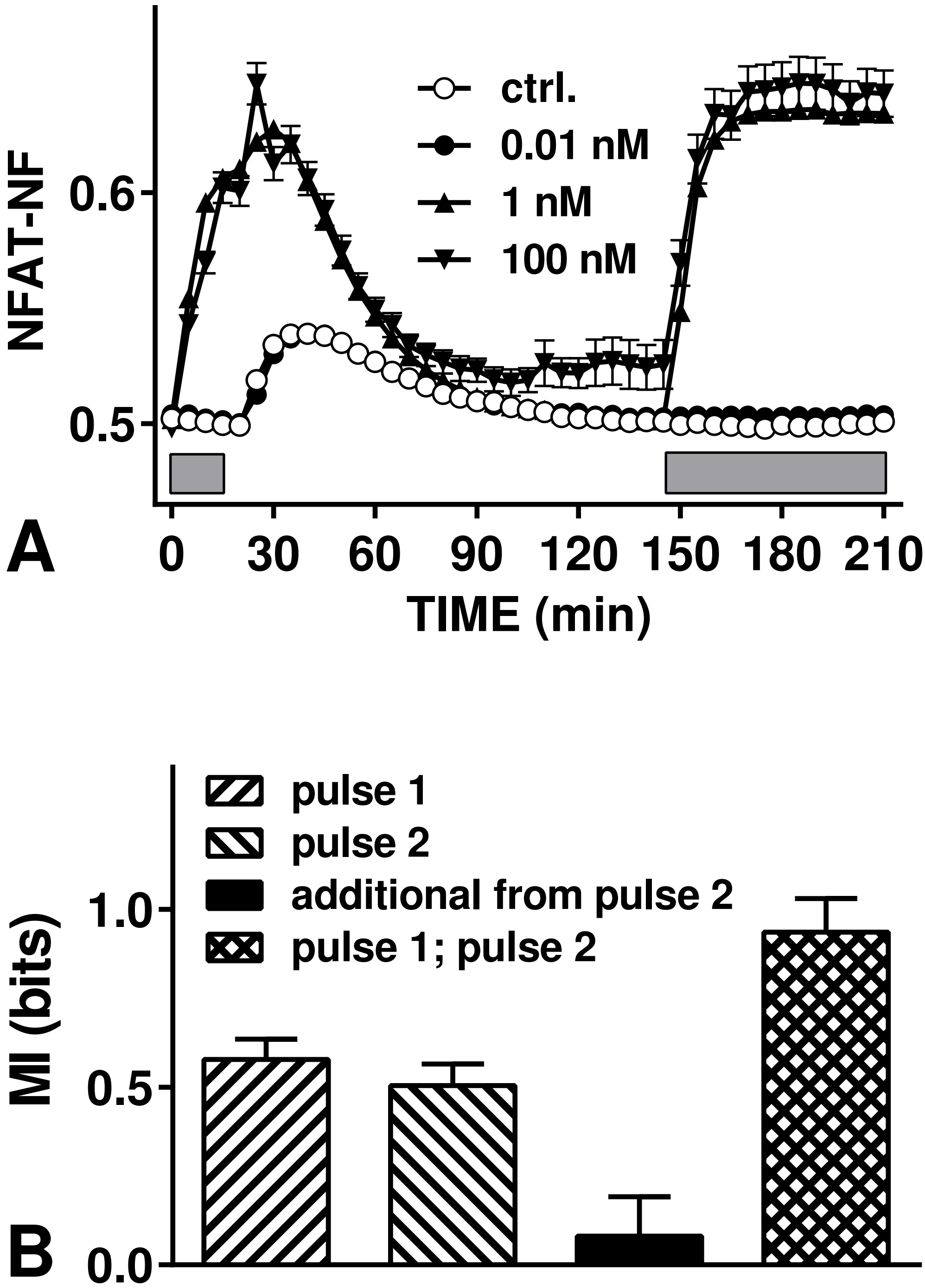

ctrl.
0.01 nM
1 nM
100 nM
NFAT-NF
0.6
0.5
A
0
30
60
90
120
150
180
210
TIME (min)
pulse 1
pulse 2
additional from pulse 2
pulse 1; pulse 2
MI (bits)
1.0
0.5
0.0
B